

Spatial distribution of stars and brown dwarfs in σ Orionis

José Antonio Caballero^{1,2}

¹*Max-Planck-Institut für Astronomie, Königstuhl 17, D-69117 Heidelberg, Germany*

²*Dpto. de Astrofísica y Ciencias de la Atmósfera, Facultad de Ciencias Físicas, Universidad Complutense de Madrid, E-28040 Madrid, Spain. E-mail: caballero@astrax.fis.ucm.es*

Accepted 2007 October –. Received 2007 October –; in original form 2007 August 13

ABSTRACT

I have re-visited the spatial distribution of stars and high-mass brown dwarfs in the σ Orionis cluster (~ 3 Ma, ~ 360 pc). The input was a catalogue of 340 cluster members and candidates at separations less than 30 arcmin to σ Ori AB. Of them, 70 % have features of extreme youth. I fitted the normalised cumulative number of objects counting from the cluster centre to several power-law, exponential and King radial distributions. The cluster seems to have two components: a dense core that extends from the centre to $r \approx 20$ arcmin and a rarified halo at larger separations. The radial distribution in the core follows a power-law proportional to r^1 , which corresponds to a volume density proportional to r^{-2} . This is consistent with the collapse of an isothermal spherical molecular cloud. The stars more massive than $3.7 M_{\odot}$ concentrate, however, towards the cluster centre, where there is also an apparent deficit of very low-mass objects ($M < 0.16 M_{\odot}$). Last, I demonstrated through Monte Carlo simulations that the cluster is azimuthally asymmetric, with a filamentary overdensity of objects that runs from the cluster centre to the Horsehead Nebula.

Key words: open clusters and associations: individual: σ Orionis – stars: formation – stars: low mass, brown dwarfs.

1 INTRODUCTION

The σ Orionis region in the Ori OB 1 b association is finally becoming recognised as one of the most important young open clusters, with an age of only about 3 Ma. In the discovery paper, Garrison (1967) used the term “clustering” to refer to an agglomeration of fifteen B-type stars surrounding and including the multiple star σ Ori. Afterwards, Lyngå (1981) tabulated σ Orionis in his catalogue of open clusters. Since the rediscovery of the cluster by Wolk (1996) and its subsequent study in depth, which has revealed the most numerous and best known substellar population (Béjar et al. 1999; Zapatero Osorio et al. 2000, 2002; Caballero et al. 2007), only a few authors have investigated the σ Orionis spatial distribution. In particular, Béjar et al. (2004) and Sherry et al. (2004) analysed the radial distribution of σ Orionis cluster members and candidates in annuli of width Δr as a function of the separation r to σ Ori AB. To maximise the number of objects per annulus and minimise the Poissonian errors, Δr must be wide. This leads to have few annuli (no more than 12 in the $r = 0$ –30 arcmin interval) to fit to a suitable radial profile (exponential decay – Béjar et al. 2004; King – Sherry et al. 2004). Both studies agree that the cluster may extend only up to ~ 25 –30 arcmin. The low surface density of cluster members at larger separations, the sharp increase of extinction due to

the nearby Horsehead Nebula-Flame Nebula-IC 434 complex and the closeness to (or even overlapping with) other stellar populations in the Orion Belt surrounding Alnitak (ζ Ori) and Alnilam (ϵ Ori) prevent from suitably broaden the radial distribution analysis (Caballero 2007a). At the canonical heliocentric distance to σ Orionis of 360 pc (e.g. Brown, de Geus & de Zeeuw 1994), the cluster would have an approximate radius of 3 pc.

In spite of the agreement on the size of σ Orionis, the fits and the profiles in Béjar et al. (2004) and Sherry et al. (2004) seem to be rather incomplete and inappropriate, respectively. On the one hand, the King models were designed for tidally truncated globular clusters (King 1962, 1966; Meylan 1987), and have also been satisfactorily used for describing galaxies (e.g. Kormendy 1977; Binggeli, Sandage & Tarenghi 1984). These systems have had enough time to be isothermal, on the contrary to very young open clusters like σ Orionis, where only gravitational relaxation by initial mixing may have occurred (King 1962). On the other hand, Béjar et al. (2004) exclusively focused on the cluster substellar population. Besides, the exponential fit in Béjar et al. (2004) only accounted for the five innermost annuli, which led to a high uncertainty in the derived parameters. Last, in the works by Sherry et al. (2004) and Béjar et al. (2004), the input list of cluster members and candidates came from

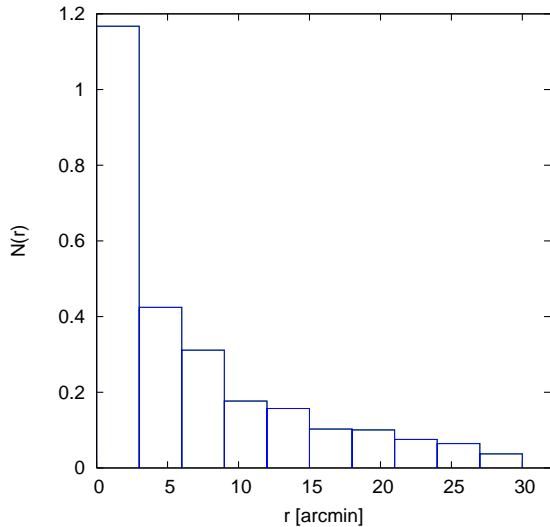


Figure 1. Binned surface density profile for σ Orionis with Caballero (2007c) data. The mean number of objects per annulus is 34 for a width $\Delta r = 3$ arcmin. All the figures are in colour in the online article on Synergy.

VRI/IZ optical surveys. Many sources in both analysis had no near-infrared or spectroscopic follow-up.

For a correct study of the spatial distribution in σ Orionis, it is therefore necessary to use new fitting radial profiles and an input catalogue as comprehensive as possible. It must cover a wide mass interval. Maximum completeness and minimum contamination of the catalogue are also desired. These requirements are verified by the *Mayrit* catalogue, which tabulates 339 σ Orionis members and candidates in a 30 arcmin-radius circular area centred on σ Ori AB (Caballero 2007c). Of them, 241 display features of extreme youth (e.g. OB spectral types, Li I in absorption, H α in strong emission, spectral signatures of low gravity, near- and mid-infrared excesses due to discs). The catalogue covers three orders of magnitude in mass, from the $\sim 18+12 M_{\odot}$ of the O9.5V+B0.5V binary σ Ori AB to the $\sim 0.033 M_{\odot}$ of the brown dwarf B05 2.03–617 (Caballero & Chabrier, in prep.). Accounting for σ Ori A and B as different objects separated by ~ 0.25 arcsec, then the equatorial coordinates of 340 young stars, brown dwarfs and cluster member candidates are available. I will use this input catalogue to investigate the radial and azimuthal distribution of objects in the σ Orionis region.

2 ANALYSIS AND RESULTS

2.1 Cluster centre and radial gradient

Caballero (2007a) showed that $\sim 46\%$ of the mass in the σ Orionis stars with $M \gtrsim 1.2 M_{\odot}$ is contained in the quintuple Trapezium-like system that gives the name to the cluster, and $\sim 29\%$ only in the AB components. This suggests using the binary as the cluster centre ($r = 0$). From the masses for the objects in the *Mayrit* catalogue derived in Caballero & Chabrier (in prep.), one third of the total cluster mass is encircled in the innermost 5 arcmin. If the mass were homogeneously distributed within the survey area, the inner-

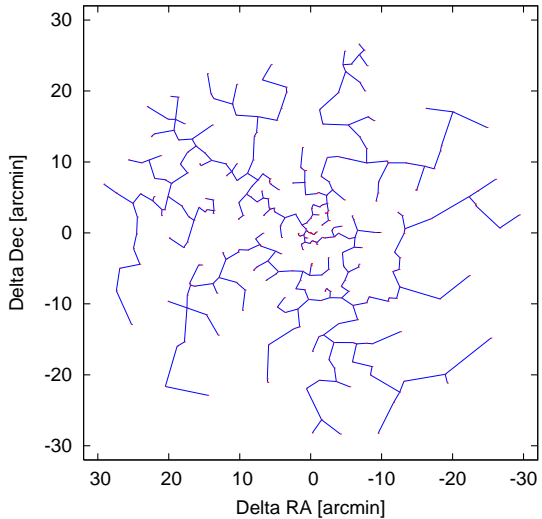


Figure 2. Euclidean minimum spanning tree for σ Orionis ($\mathcal{Q} \approx 0.88$). I have used a MATLAB/OCTAVE function based on an open code by F. W. J. van der Berg (University of Copenhagen), based in its turn on an algorithm by Hillier and Lieberman (2001). The minimum spanning trees for ρ Ophiuchus, IC 2391, IC 348, Taurus and Chamaeleon are shown in Cartwright & Whitworth (2004).

most 5 arcmin would contain only 2.8% of the total cluster mass [$(5/30)^2 \approx 0.028$]. I will consider σ Ori AB as the origin of coordinates because of: (i) simplicity (the coordinates of the binary are well determined by *Hipparcos*; the actual coordinates of the cluster barycentre may change when a different input list of cluster members and individual masses is used); (ii) reflection of the geometry of the *Mayrit* survey in Caballero (2007c), which was centred on σ Ori AB; and (iii) uniformity with previous works (especially with Béjar et al. 2004 and Sherry et al. 2004, who also used σ Ori AB as the coordinate origin). There might be an additional reason: the largest mass aggregation is probably associated to the densest region of the original molecular cloud where the fragmentation and star formation initiated (assuming that the origin of the reference frame is locked to the –moving– cluster barycentre). This reason may be unconvincing, because highly turbulent (and fractal-like?) molecular clouds probably do not have a “centre” that can be defined in any sensible way, as shown in the simulations of Bonnell, Bate & Vine (2003). See Section 2.4 in this work and fig. 1 in Caballero (2007a) for pictorial views of the spatial distribution of confirmed and candidate cluster members in the σ Orionis region, and Caballero (2007b) for a description of the cluster centre. The old-fashioned plot of the surface density is shown in Fig. 1; see similar plots in Sherry et al. (2004) and Béjar et al. (2004) for comparison.

There exists a \mathcal{Q} -parameter which quickly, and simply, shows if a distribution of cluster members is smooth (a large-scale radial density gradient) or clumpy a (multiscale fractal subclustering; Cartwright & Whitworth 2004). The \mathcal{Q} -parameter is defined by:

$$\mathcal{Q} = \frac{\overline{m}}{s}, \quad (1)$$

where m and s are the edge length of the Euclidean minimum spanning tree and the separation between cluster mem-

bers, respectively. A minimum spanning tree is a network (“graph”) of $N_{\max}-1$ lines (“edges”) that connect the N_{\max} objects (“nodes”) in the shortest possible way under the condition no closed loops allowed. See, e.g., Graham, Clowes & Campusano (1995) for an application of minimum spanning trees in Astrophysics¹. The normalization factors are $(N_{\max}\pi r_{\max}^2)^{1/2}/(N_{\max}-1)$ and r_{\max} for m and s (N_{\max} is the total number of cluster members and πr_{\max}^2 is the area of the circular survey).

For the 340 σ Orionis cluster member and candidates, I have measured $\overline{m} = 0.589$ and $\overline{s} = 0.668$. Therefore, the Cartwright & Whitworth (2004) parameter is $\mathcal{Q} \approx 0.88$. This value is larger than 0.80, which distinguish σ Orionis as a cluster with a smooth large-scale radial density gradient and a moderate degree of central concentration. This concentration is larger than in ρ Ophiuchus, other cluster with a radial density gradient, but less than in IC 348 (Cartwright & Whitworth 2004). Other sparse clusters and star-forming regions, like IC 2391, Taurus and Chamaeleon, have \mathcal{Q} -parameters in the interval 0.47–0.67, which indicates that they have, on the contrary, substructure with fractal dimensions between 1.5 and 2.5.

2.2 Surface density and cumulative number of objects

I present an innovative, accurate, simple method to derive the actual expression of the surface density as a distance from the cluster centre, $\sigma(r)$. It can be applied to other open and globular clusters and galaxies. The normalised cumulative number of objects counting from the cluster centre, $f(r)$, is:

$$f(r) = \frac{N(r)}{N(r_{\max})}, \quad (2)$$

where $N(r)$ is the total number of stars in projection within a distance r of the centre. If there is azimuthal symmetry, $N(r)$ is related to the surface density through the following expression:

$$N(r) = 2\pi \int_0^r dr' r' \sigma(r'). \quad (3)$$

The relatively high value of the \mathcal{Q} -parameter of σ Orionis supports the hypothesis of azimuthal symmetry in this cluster in particular. For systems without azimuthal symmetry (e.g. elliptical galaxies), use instead:

$$N(r) = \int_0^r \int_0^{2\pi} dr' d\theta r' \sigma(r', \theta). \quad (4)$$

The surface $\sigma(r)$ and volume $\rho(r)$ densities are linked through the simple relation $\sigma(r) = 2r\rho(r)$. This equality comes from:

$$N(r) = 4\pi \int_0^r dr' r'^2 \rho(r') = 2\pi \int_0^r dr' r' \sigma(r') \quad [\forall r], \quad (5)$$

assuming again azimuthal symmetry². The function $f(r)$ varies from 0 at $r = 0$ to 1 at $r = r_{\max}$. In the *Mayrit* survey, $r_{\max} = 30$ arcmin and $N(r_{\max}) (\equiv N_{\max}) = 340$. In the discrete approximation, $N(r) \approx N^*(r)$ and:

$$f(r) \approx f^*(r) = \frac{\sum_{i=1}^{N^*(r)} i}{\sum_{i=1}^{N(r_{\max})} i} = \frac{N^*(r)}{N_{\max}}. \quad (6)$$

I have investigated several functional expressions of $\sigma(r)$ that fit in more or less degree the observed normalised cumulative number of objects, $f^*(r)$. A general expression for a power-law surface density of index $\delta - 2$ is:

$$\sigma(r, \delta) = \frac{\delta N_{\max} r^{\delta-2}}{2\pi r_{\max}^{\delta}}, \quad (7)$$

which, after integration, leads to a simple expression for $f(r)$:

$$f(r, \delta) = \left(\frac{r}{r_{\max}}\right)^{\delta}. \quad (8)$$

In this approach, the objects are uniformly distributed in a circular area if $\delta = 2$ ($\sigma = \text{constant}$). Surface densities with parameter $\delta < 0$, that predict a lower number of objects close to the centre, were obviously not considered.

Following Béjar et al. (2004), I have also studied two expressions of exponential decay of the surface density:

$$\sigma(r, \epsilon) = \sigma_0 e^{-\epsilon r} \quad (9)$$

$$\sigma_0 = \frac{N_{\max}}{2\pi} \frac{1}{\frac{1}{\epsilon^2} - e^{-\epsilon r_{\max}} \left(\frac{1}{\epsilon^2} + \frac{r_{\max}}{\epsilon}\right)} \quad (10)$$

$$f(r) = \frac{1 - e^{-\epsilon r}}{1 - e^{-\epsilon r_{\max}}} \quad (11)$$

and:

$$\sigma(r, \epsilon) = \sigma_0 e^{-\epsilon r^2} \quad (12)$$

$$\sigma_0 = \frac{\epsilon N_{\max}}{\pi} \frac{1}{1 - e^{-\epsilon r_{\max}^2}} \quad (13)$$

$$f(r) = \frac{1 - e^{-\epsilon r^2}}{1 - e^{-\epsilon r_{\max}^2}}. \quad (14)$$

Finally, I have also investigated the King (1962) profile for gravitationally relaxed globular clusters. Close to the centre, the surface density can be expressed by:

$$\sigma(r) \approx \sigma_c(r) = \frac{\sigma_0}{1 + (r/r_c)^2}, \quad (15)$$

where r_c is the core radius and σ_0 is the central surface density. In the limit of the cluster, the surface density is:

$$\sigma(r) \approx \sigma_t(r) = \sigma_1 \left(\frac{1}{r} - \frac{1}{r_t}\right)^2, \quad (16)$$

where r_t is the tidal radius (the value of r at which $\sigma_t(r)$ reaches zero) and σ_1 is a constant. The overall normalised cumulative number of objects that embodies $\sigma_c(r)$ and $\sigma_t(r)$ is, following the nomenclature by King (1962):

² Cartwright & Whitworth (2004) demonstrated that the equality is based on a fallacious assumption. The differences between $\sigma(r)$ and $2r\rho(r)$, linked to distribution functions of type 2D1 and 3D2 in the nomenclature by those authors, are, however, too small to be considered in this work.

¹ The first algorithm for finding a minimum spanning tree was developed to find an efficient electrical coverage of Czech Moravia (Borůvka 1926)

$$f(r) = \frac{\log(1+x) - 4 \frac{(1+x)^{1/2} - 1}{(1+x_t)^{1/2}} + \frac{x}{1+x_t}}{\log(1+x_{\max}) - 4 \frac{(1+x_{\max})^{1/2} - 1}{(1+x_t)^{1/2}} + \frac{x_{\max}}{1+x_t}}, \quad (17)$$

where $x = (r/r_c)^2$, $x_t = (r_t/r_c)^2$ and $x_{\max} = (r_{\max}/r_c)^2$.

Fig. 3 illustrates the fits of $f(r)$ to $f^*(r)$ to evaluate the most suitable expression for $\sigma(r)$. The best match for a simple power-law density is acquired for $\delta = 0.9$. Power-laws with $\delta \gg 1$ and $\delta \ll 1$ provide inaccurate fits. Likewise, the exponential profiles cannot predict the large actual surface density close to the cluster centre (the binned surface density profile in Fig. 1, when plotted in logarithmic scale, also shows that the innermost bin deviates from the exponential profile). The overall King profile has the same problem. I performed intensive computations, not shown here, to cover the (r_t, r_c) parameter space of the King profile. No clear minimum of the χ^2 exists for the σ Orionis radial distribution when fitted to the King empirical density law. The best solutions were found for all the combinations that satisfy $r_c = 8\text{--}12$ arcmin and $r_t \gg r_c$. The excesses of light at large radii of young massive clusters with respect to King (and Elson, Fall & Freeman 1987) profile(s), attributed to gas expulsion by Goodwin & Bastian (2006), cannot explain the poor fitting for the King profile at small radii in σ Orionis.

The best general fit is obtained for a composite power-law, as shown in Fig. 4. The cumulative number of σ Orionis objects grows proportional to r (i.e. $\delta = 1.0$) up to ~ 20 arcmin. This size translates into a physical radius of ~ 2 pc. At larger separations, $f(r)$ increases with a lower slope, indicating an exponent $\delta \approx 0.7$. In reality, at such separations, an exponential or a limit King [$\sigma_t(r)$] profile would also fit the data. From the extrapolation of the $f(r) \propto r$ law up to the radius of 30 arcmin, there is deficit of 30–40 objects in the outermost annulus. As a result, the σ Orionis cluster may be spatially described as a central ($r \lesssim 20$ arcmin), dense region –the “core”– and an outer ($r \gtrsim 20$ arcmin), more rarified region –the “halo”–. From these data, the power-law index transition between the core and the halo is quite smooth. However, the relative drop of $f(r)$ at $r \sim 20$ arcmin might be more or less abrupt because of our poor knowledge of the σ Orionis stellar population at large separations from the cluster centre. As an example, while more than 90% of cluster members and candidates of the *Mayrit* catalogue in the innermost 10 arcmin have known features of extreme youth, this ratio is about 50% in the halo (past spectroscopic, mid-infrared and X-ray analysis have been naturally focused on the cluster centre and its surroundings). Going deeply into this subject seems to be meaningless because of the relatively small amount of investigated cluster objects in the halo, contamination by young neighbouring stellar populations in Orion (Jeffries et al. 2006; Caballero 2007a) or fore-/background stars (e.g. Caballero, Burgasser & Klement, in prep.), variable extinction to the northeast of the survey area, incompleteness of the *Mayrit* catalogue (Caballero 2007c) and the “anomalous” radial distribution discussed next.

The radial distribution of the cluster core is, on the contrary to the halo, free of possible systematic errors. The $f(r) \propto r$ law in the core is translated to surface and volume densities $\sigma(r) \propto r^{-1}$ and $\rho(r) \propto r^{-2}$. Radial profile investigations carried out in other very young star-forming regions

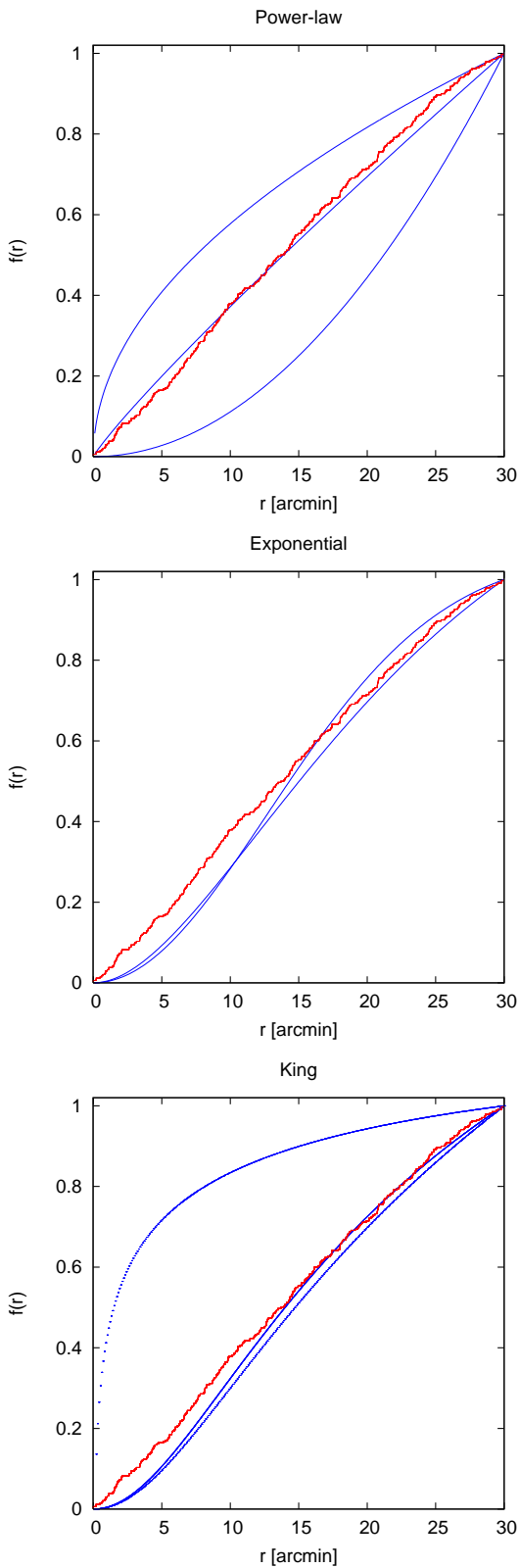


Figure 3. Normalised cumulative number of σ Orionis objects, $f^*(r)$, in (red) steps plot style and theoretical distribution in (blue) solid line. *Top panel:* power-law distributions for $f(r) \propto r^{1/2}$, $r^{0.9}$, r^2 (from top to bottom); *middle panel:* exponential distributions for $\sigma(r) \propto e^{-\epsilon r}$ ($\epsilon = 1/12$ arcmin $^{-1}$) and $e^{-\epsilon r^2}$ ($\epsilon = 1/18^2$ arcmin $^{-2}$); *bottom panel:* King distributions for the core, limit (dotted) and overall radial profiles ($r_c = 10$ arcmin, $r_t = 200$ arcmin).

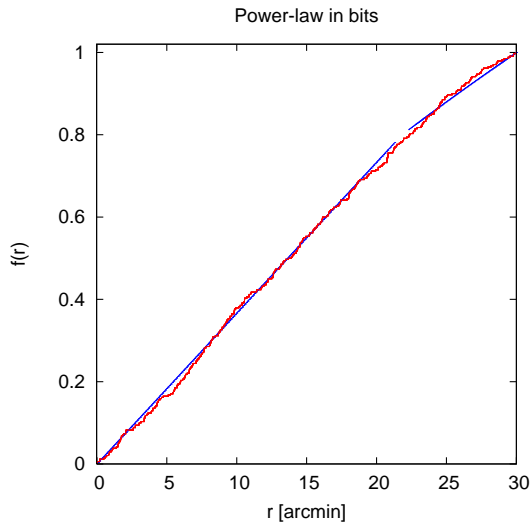


Figure 4. Same as Fig. 3 but for a composite theoretical distribution with $f(r) = 1.1 \left(\frac{r}{r_{\max}}\right)^{1.0}$ for $r < 21$ arcsec and $f(r) = 1.0 \left(\frac{r}{r_{\max}}\right)^{0.7}$ for $r > 23$ arcsec.

have found similar distributions. Not far away from σ Orionis, Bate, Clarke & McCaughrean (1998) noticed that the stars of the Orion Nebula Cluster are distributed with a core of uniform volume density and radius $r_{\text{core}} = 0.5$ arcmin and a volume density profile $\rho(r) \propto r^{-2}$ at larger separations. Alike power-law volume density distributions have been found in other star-forming regions, like Taurus (Fuller & Myers 1992; Ward-Thompson et al. 1994), or low-mass cold dark molecular clouds, like Barnard 68 (Alves, Lada & Lada 2001). Furthermore, the power-law index 2 is an “often-used initial condition for numerical calculations of star formation” (Burkert, Bate & Bodenheimer 1997). The $\rho(r) \propto r^{-2}$ distribution corresponds to a singular, self-gravitating, (rotating) isothermal sphere. Finally, from fig. 5 in Cartwright & Whitworth (2004) and the Q -parameter value for σ Orionis derived in Section 2.1, I estimate that the volume density in the cluster varies as $\rho(r) \propto r^{-1.7 \pm 0.4}$. The -1.7 ± 0.4 index is intermediate between those in ρ Ophiuchus (-1.2) and IC 348 (-2.2) and consistent with $\rho(r) \propto r^{-2}$.

The use of the power-law function $f(r) \propto r$, whose corresponding $\sigma(r)$ diverges at $r = 0$, has the drawback of an incorrect fit in the innermost 1 arcmin of the cluster. Characterising the very centre of the cluster is out of the scope of this work, since it can be only accomplished with high spatial-resolution facilities (e.g. adaptive optics or mid-infrared instruments – van Loon & Oliveira 2003; Caballero 2005). Moreover, the Bate et al. (1998)’s value of r_{core} can be suitably applied to σ Orionis. There are only seven stars at less than 0.5 arcmin to σ Ori AB (Caballero 2007b), so the central surface density is $\sigma_0 \approx 9 \text{ arcmin}^{-2}$. This value matches well with the actual value of $\sigma(r_{\text{core}})$ for $f(r) \propto r$. The observational parallelism between the radial distributions of the Orion Nebula Cluster and other star-forming regions and of σ Orionis evidences that the collapse of an isothermal cloud to form a star cluster might be universal.

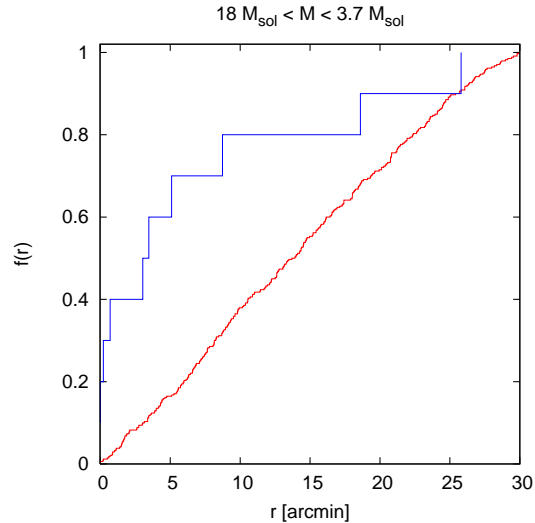


Figure 5. Mass-dependent normalised cumulative number of high-mass σ Orionis stars as a function of the separation to the cluster centre. The observed $f^*(r)$ for the 340 objects is overplotted as in Figs. 3 and 4.

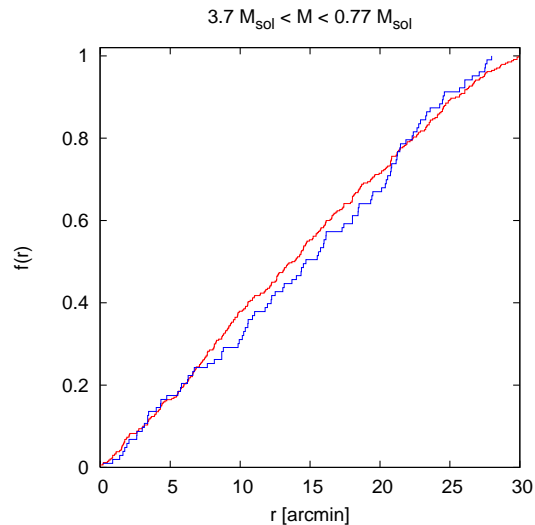


Figure 6. Same as Fig. 5, but for intermediate-mass stars.

2.3 Mass-dependent radial distribution

I have also investigated the radial profile of σ Orionis cluster members and candidates for different mass intervals. I have separated the 340 stars and brown dwarfs in four mass groups that are equally spaced in logarithmic scale. The boundaries between the groups are at about 3.7, 0.77 and $0.16 M_{\odot}$. The groups contain, from the most to the least massive, 10, 103, 155 and 72 elements. Figs. 5 to 8 show the normalised cumulative number of objects for the four groups compared to the average distribution. It is manifest that the ten stars more massive than $3.7 M_{\odot}$ depart from the general trend $f(r) \propto r$, while the brown dwarfs and stars below this mass roughly follow it. The massive stars seem to obey the King profile close to the cluster centre (with a surface density $\sigma_c(r) = \frac{f_0}{1+(r/r_c)^2}$) rather than a power-law, whose

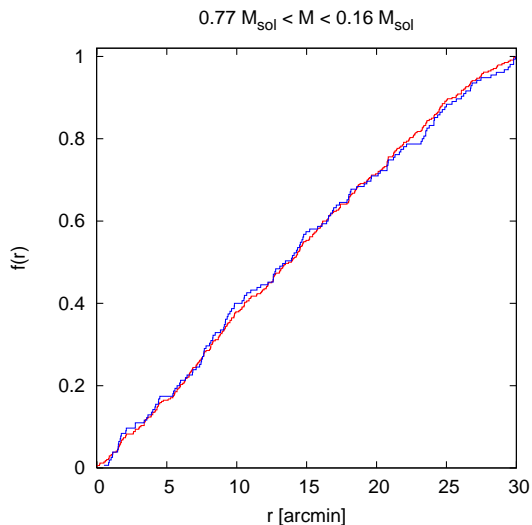


Figure 7. Same as Fig. 5, but for low-mass stars.

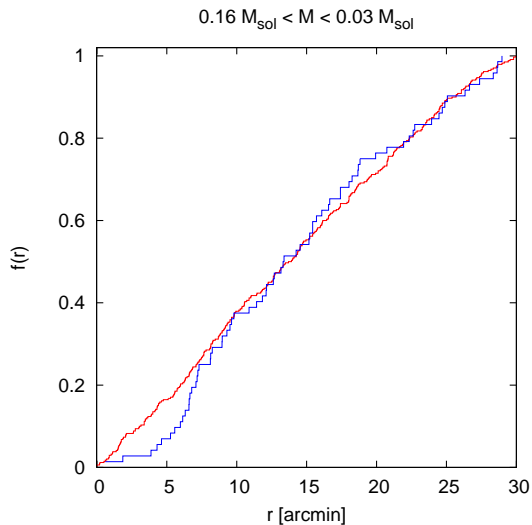


Figure 8. Same as Fig. 5, but for very low-mass stars and brown dwarfs. Note the deficit of very low-mass cluster member and candidates at $r \lesssim 4$ arcmin and the inclined raise at $r = 6-7$ arcmin

exponent should be as low as $\delta \sim 0.1$. Eight of the ten most massive σ Orionis stars are, besides, within the 10 arcmin-radius circle. This agglomeration of early-type stars towards the cluster centre is typical in other very young star-forming regions, such as the Orion Nebula Cluster, whose centre is defined by the OB-type stars of the θ^1 Ori multiple system. This result shows again the resemblance between both Orion clusters.

There is no other characteristic feature in the mass-dependent distribution in Figs. 5 to 8, except for a remarkable deficit of very low-mass stars and high-mass brown dwarfs ($0.16 M_{\odot} \leq M \leq 0.03 M_{\odot}$) in the innermost 4 arcmin together with a steep raise of $f^*(r)$ at 6–7 arcmin (Fig. 8). On the one hand, there are only two representatives of this mass interval within 4 arcmin: Mayrit 36273 and the Class I object Mayrit 111208. Both of them are the faintest

sources with I -band photometry identified in the near-infrared/optical/X-ray survey in the centre of σ Orionis by Caballero (2007b). On the other hand, there are almost 20 low-mass stars and brown dwarfs in the narrow annulus 5–8 arcmin. An $0.16 M_{\odot}$ -mass object in the cluster, in the upper limit of low-mass interval, has typical magnitudes $I \sim 16.0$ mag, $J \sim 14.0$ mag. These values are far brighter than the DENIS and 2MASS completenesses, even in the innermost region affected by the glare of the multiple system σ Ori. Caballero (2007b) failed to confirm or refute this absence of very low-mass stars and high-mass brown dwarfs. The raise of $f^*(r)$ at 6–7 arcmin indicates, on the contrary, a larger density of very low-mass objects in this annulus. One can think of many ways which could give rise to the deficit of low-mass objects at small radii and excess at intermediate radii. Firstly, low-mass objects could actually form in the 6–7 arcmin annulus and not in the inner regions (maybe core masses were higher in the centre, or competitive accretion caused central brown dwarfs to grow into stars). Alternatively, they could form in the cluster centre, but were ejected via dynamical interactions with the massive stars. Low-mass objects do not have enough energy, however, to move further away from the deep σ Ori gravity well of $M > 50 M_{\odot}$. The deficit-excess needs to be explained by theory, but this particular set of observations does not give any indication of a preferred formation scenario [see Whitworth et al. (2007) for a review on the theory of formation of brown dwarfs and very low-mass stars]. Further and innovative observations, able to avoid the extense glare of the OB system, are required to determine if the peculiar distribution of very low-mass objects in the cluster centre are due to an observational bias or to an actual consequence of the formation mechanism. Some observational efforts on this topic have been carried out by Caballero (2005, 2007b) and Sherry, Walter & Wolk (2005).

2.4 Azimuthal asymmetry

Top window in Fig. 9 shows that the distribution of confirmed cluster members and candidates is not whole radially symmetric, with an evident lower density to the west of σ Ori AB with respect to the east. An elongated subclustering is manifest to the east-northeast of the cluster centre, just in the direction to the Horsehead Nebula. On the contrary, Béjar et al. (2004) derived that the variation of the radial distribution of their very-low mass stars and brown dwarfs over their best exponential law fit was Poissonian, implying no evidence of subclustering. The object sample presented in this paper surpasses Béjar et al.’s one and allows to corroborate or invalidate their statement.

I have looked for an azimuthal asymmetry in the σ Orionis cluster in several steps. First, I have generated 1000 simulated distributions³ following the power law $f(r) = \left(\frac{r}{r_{\max}}\right)^{1.0}$. Ten of them (one is highlighted) are shown in the bottom window in Fig. 9. The resemblance with the actual distribution, in the top window of the Figure, is evident. Second, I have divided the survey area in nine regions:

³ In the general power-law distribution case with index δ , if \mathbf{r} is a vector of length N_{\max} of uniformly distributed pseudo-random radii between $r = 0$ and r_{\max} , then the distribution of the vector $\mathbf{r}^{1/\delta}$ follows $f(r) = \left(\frac{r}{r_{\max}}\right)^{\delta}$.

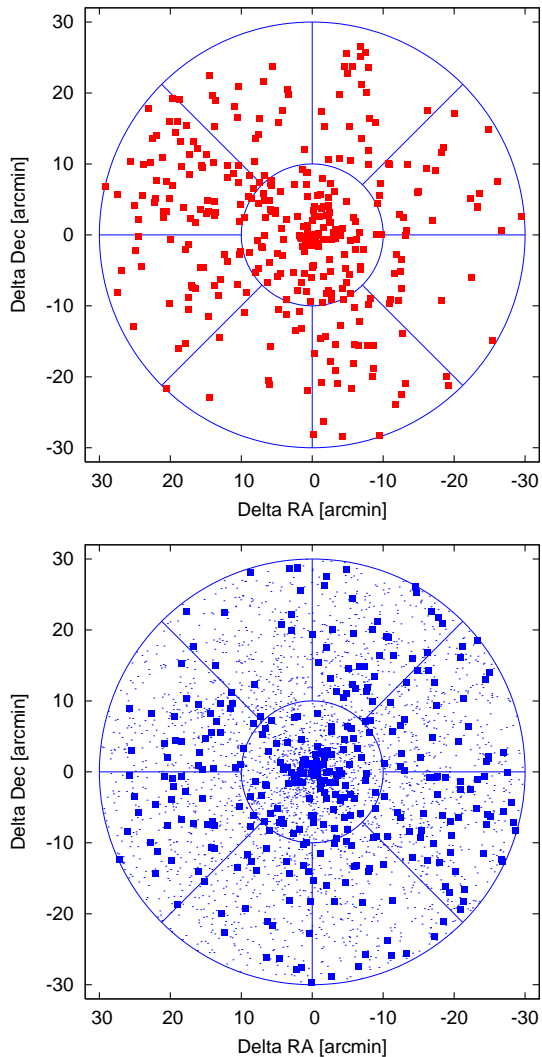


Figure 9. Actual (top) and simulated (bottom) spatial distributions of σ Orionis objects in the survey area. The coordinate origin is in σ Ori A. The bottom window shows 10 Monte Carlo simulations following $f(r) = \left(\frac{r}{r_{\max}}\right)^{1.0}$. One distribution is marked with small filled squares, the remaining ones are marked with points. The sizes of the small and big solid circles are 10 and 30 arcmin. The eight equal-size segments of annuli used for the computation of the asymmetry factor, ζ , are also indicated.

a central area, 10-arcmin wide, where the asymmetry is difficult to quantify, and eight segments of the annulus in the radius interval $10 \text{ arcmin} < r < 30 \text{ arcmin}$. Third, for each simulated distribution, I have computed its corresponding asymmetry factor, ζ , defined by:

$$\zeta = \frac{(N_1 + N_2) - (N_7 + N_8)}{N_{\max}}, \quad (18)$$

where N_1 and N_2 are the numbers of objects of the two most populated segments of annulus, and N_7 and N_8 are those of the less populated. The mean and the standard deviation of the 1000 computed asymmetry factors are $\bar{\zeta} = 0.0698$, $\sigma_{\zeta} = 0.0189$. The maximum and minimum asymmetry factors are $\zeta_{\max} = 0.1382$ and $\zeta_{\min} = 0.0176$. The four values ($\bar{\zeta}$, σ_{ζ} , ζ_{\max} and ζ_{\min}) are faultless compatible with the Poissonian errors within each segment of annulus. Fi-

nally, I have measured the asymmetry factor for the actual σ Orionis distribution: $\zeta^* = 0.1853$. This value deviates 6.1 times the σ_{ζ} from the $\bar{\zeta}$ and is significantly larger than the ζ_{\max} among 1000 Monte Carlo simulations. Considering as a first order of approximation that the values ζ_i ($i = 1 \dots 1000$) are distributed following a standard normal distribution with parameters $\bar{\zeta}$ and σ_{ζ} , then there is a probability $p = 1 - \text{erf}(6.1/2^{1/2}) \approx 10^{-9}$ (where “erf” is the error function) that the actual value ζ^* follows such distribution. Even accounting for generous systematic errors or biases, it is highly probable that the radial distribution of objects at more than 10 arcmin from the centre of σ Orionis is azimuthally asymmetric.

The most populated segments of annulus of the actual distribution are, counting anti-clockwise from 12 hours, the second (coinciding with the elongated subclustering in the direction to the Horsehead Nebula) and the fifth ones. Both two segments and the cluster centre spatially coincide with a filamentary region of maximum emission at the $12 \mu\text{m}$ *IRAS* passband (see fig. 2 in Oliveira & van Loon 2004). This “warmer” region has not been identified in works based on recent observations with IRAC and MIPS onboard *Spitzer* (e.g. Hernández et al. 2007) or with the Spatial Infrared Imaging Telescope on the Midcourse Space Experiment satellite (Kraemer et al. 2003). From my data, I cannot postulate whether the largest surface density of σ Orionis objects originally arises from an hypothetical larger density of warm dust in the region or, inversely, the filamentary region is a consequence of both the low spatial resolution imaging capabilities of *IRAS* and the largest surface density of objects (i.e. the red σ Orionis objects, many with mid-infrared excesses due to discs –Oliveira et al. 2006; Hernández et al. 2007; Caballero et al. 2007–, generate a smooth background at $12 \mu\text{m}$ that *IRAS* was not able to resolve).

The accumulation of stars and brown dwarfs in a filamentary pattern in σ Orionis strongly supports some star formation scenarios of collapse and fragmentation of a large-scale turbulent molecular cloud, especially those that predict burst of star formation in filamentary gas (e.g. Bate, Bonnell & Bromm 2003). It is stimulating to notice that these simulations assumed the contraction of an isothermal, spherical molecular cloud with $\rho(r) \propto r^{-2}$ (see Section 2.2). The filamentary accumulation in σ Orionis is, however, peculiar, because no similar arrangements have been found in other star-forming regions. For example, Gómez et al. (1993) and Larson (1995) found that the subclustering in Taurus-Auriga is in the form of star clumps of ~ 15 components, while Bate et al. (1998) showed that in the Orion Nebula Cluster there is no subclustering at all. It is obvious that further investigations are needed; percolation or two-point correlation function of stars are different approaches that can be used.

3 SUMMARY

The $\sim 3 \text{ Ma}$ -old σ Orionis cluster is a perfect laboratory of star formation. I have investigated the radial distribution of 340 cluster members and candidates in a 30 arcmin-radius area centred on σ Ori AB, taken from Caballero (2007c). The analysis has covered a mass interval from the $18+12 M_{\odot}$ of σ Ori AB to the $\sim 0.03 M_{\odot}$ of the faintest brown dwarf detectable by DENIS. The cluster shows a clear radial density

gradient, quantified by the \mathcal{Q} -parameter, that accounts for the mean separation between members and the Euclidean minimum spanning tree of the cluster. I have calculated the functional relations between normalised cumulative numbers of objects counting from the cluster centre, $f(r)$, and surface densities, $\sigma(r)$. Cumulative distribution functions as these avoid many problems associated with binning. Among the studied radial (power-law, exponential and King) profiles, the best fit is for a composite power-law distribution of cluster members with a core and a rarified halo. The core extends up to ~ 20 arcmin from the cluster centre and is nicely modelled by a surface density $\sigma(r) \propto r^{-1}$, that corresponds to a volume density $\rho(r) \propto r^{-2}$. This volume density matches, in its turn, the radial profile in a cluster formed from the collapse of a self-gravitating, isothermal sphere. The most massive σ Orionis stars deviate, however, from the general trend and are much more concentrated towards the cluster centre. There is also an apparent deficit of very low-mass stars and high-mass brown dwarfs ($0.16 M_{\odot} \gtrsim M \gtrsim 0.035 M_{\odot}$) in the innermost 4 arcmin and an excess in the annulus at 6–7 arcmin to the central Trapezium-like system. Last, there is a significant azimuthal asymmetry due to a filament-shape overdensity of objects that connects the cluster centre with a part of the Horsehead Nebula. This discovery supports the formation scenarios that predict burst of star formation in filamentary gas.

ACKNOWLEDGMENTS

I thank the anonymous referee for helpful comments. J.A.C. was formerly an Alexander von Humboldt Fellow at the MPIA, and is currently an Investigador Juan de la Cierva at the UCM. Partial financial support was provided by the Universidad Complutense de Madrid and the Spanish Ministerio Educación y Ciencia under grant AyA2005–02750 of the Programa Nacional de Astronomía y Astrofísica and by the Comunidad Autónoma de Madrid under PRICIT project S–0505/ESP–0237 (AstroCAM).

REFERENCES

- Alves J. F., Lada C. J., Lada E. A. 2001, *Nature*, 409, 159
 Bastian N., Goodwin S. P., 2006, *MNRAS*, 369, L9
 Bate M. R., Clarke C. J., McCaughrean, M. J., 1998, *MNRAS*, 297, 1163
 Bate M. R., Bonnell I. A., Bromm V., 2003, *MNRAS*, 339, 577
 Béjar V. J. S., Zapatero Osorio, M. R., Rebolo, R., 1999, *ApJ*, 521, 671
 Béjar V. J. S., Caballero J. A., Rebolo R., Zapatero Osorio M. R., Barrado y Navascués D., 2004, *Ap&SS*, 292, 339
 Binggeli B., Sandage A., Tarengi M. 1984, *AJ*, 89, 64
 Bonnell I. A., Bate M. R., Vine S. G., 2003, *MNRAS*, 343, 413
 Borůvka O., 1926, *Práce mor. přírodověd. spol. v Brně III*, 3, 37
 Brown A. G. A., de Geus E. J., de Zeeuw P. T., 1994, *A&A*, 289, 101
 Burkert A., Bate M. R., Bodenheimer P., 1997, *MNRAS*, 289, 497
 Caballero J. A., 2005, *Astron. Nachr.*, 326, No. 10, 1007
 Caballero J. A., 2007a, *A&A*, 466, 917
 Caballero J. A., 2007b, *AN*, 328, 917
 Caballero J. A., 2007c, *A&A*, submitted
 Caballero J. A., Béjar V. J. S., Rebolo R. et al. 2007, *A&A*, 470, 903
 Cartwright A., Whitworth A. P., 2004, *MNRAS*, 348, 589
 Elson R. A. W., Fall M. S., Freeman K. C., 1987, *ApJ*, 323, 54
 Garrison R. F. 1967, *PASP*, 79, 433
 Gómez M., Hartmann L., Kenyon S. J., Hewett R., 1993, *AJ*, 105, 1927
 Hernández J., Hartmann L., Megeath T. et al., 2007, *ApJ*, 662, 1067
 Hiller F. S., Lieberman G. J., 2001, *Introduction to Operations Research*, 7th edition, McGraw-Hill College, ISBN 0072321695
 Jeffries R. D., Maxted P. F. L., Oliveira J. M., Naylor T., 2006, *MNRAS*, 371, L6
 Kenyon M. J., Jeffries R. D., Naylor T., Oliveira J. M., Maxted P. F. L., 2005, *MNRAS*, 356, 89
 King I., 1962, *AJ*, 67, 47
 King I., 1966, *AJ*, 71, 64
 Kormendy J., 1977, *ApJ*, 218, 333
 Kraemer K. E., Shipman R. F., Price S. D., Mizuno D. R., Kuchar T., Carey S. J., 2003, *AJ*, 126, 1423
 Larson R. B., 1995, *MNRAS*, 272, 213
 van Loon J. Th., Oliveira J. M., 2003, *A&A*, 405, L33
 Lyngå G., 1981, *The Catalogue of Open Star Clusters*, AD-CBu, 1, 90
 Meylan G., 1987, *A&A*, 184, 144
 Oliveira J. M., van Loon J. Th., 2004, *A&A*, 418, 663
 Oliveira J. M., Jeffries R. D., van Loon J. Th., Rushton M. T., 2006, *MNRAS*, 369, 272
 Sherry W. H., Walter F. M., Wolk S. J., 2004, *AJ*, 128, 2316
 Sherry W. H., Walter F. M., Wolk S. J., 2005, *Protostars and Planets V*, Proceedings of the Conference held October 24–28, 2005, in Hilton Waikoloa Village, Hawai'i. LPI Contribution No. 1286., p.8599
 Ward-Thompson D., Scott P. F., Hills R. E. & Andre P., 1994, *MNRAS* 268, 276
 Whitworth A. P., Bate M. R., Nordlund Å., Reipurth Bo, Zinnecker H., 2007, *Protostars and Planets V*, Bo Reipurth, D. Jewitt, and K. Keil (eds.), University of Arizona Press, Tucson, 459–476
 Wolk S. J., 1996, Ph.D. thesis, State Univ. New York at Stony Brook
 Zapatero Osorio M. R., Béjar V. J. S., Martín E. L., Rebolo R., Barrado y Navascués D., Bailer-Jones C. A. L., Mundt R., 2000, *Science*, 290, 103
 Zapatero Osorio M. R., Béjar V. J. S., Martín E. L., Rebolo R., Barrado y Navascués D., Mundt R., Eislöffel J., Caballero J. A., 2002, *ApJ*, 578, 536

This paper has been typeset from a $\text{\TeX}/\text{\LaTeX}$ file prepared by the author.